

# Hydraulic barrier performance of fiber-reinforced cement treated clay in large strain states

Kotake, N. & Kamon, M.

*Kagawa National College of Technology, Kagawa, Japan*

Takeuchi, N.

*Toyota Boshoku Corporation (Formerly graduate student of Kyoto University)*

Inui, T. & Katsumi, T.

*Graduate School of Global Environmental Studies, Kyoto University, Kyoto, Japan*

Keywords: fiber reinforced geomaterial, hydraulic barrier performance, toughness, triaxial compression

ABSTRACT: Hybrid clay barrier (HCB) is a fiber-reinforced geomaterial developed for barrier system of coastal landfill sites and has a feature to improve toughness of brittle cement treated clay (CTC) by inclusion of polymeric fibers. HCB consists of clay processed to slurry, hardening agent and polymeric fibers. HCB is expected to keep sufficient hydraulic barrier performance when it is subjected to large deformation associated with earthquake motions and settlements of the soft foundation ground. In the present study, to clarify quantitatively the hydraulic barrier performance of HCB in relation to strain levels, a series of hydraulic conductivity tests were conducted on HCB specimens that had suffered from relatively large strains in triaxial compression states. From the test results it can be observed that the hydraulic conductivity values of HCB increased by one order after the peak states, and then kept in the similar range even when the axial strains increased to the range up to 15%, while those of CTC showed a rapid increase under the low confining pressure in loading.

## 1 INTRODUCTION

Hybrid clay barrier (HCB) is a fiber-reinforced cement treated clay developed for barrier system of coastal landfill sites and has a feature to improve toughness of brittle cement treated clay (CTC) by inclusion of polymeric fibers. HCB is a composite geo-material consisting of dredged marine clay with high water content, hardening agent and polymeric fibers. Therefore, the mixing proportion of HCB should be properly defined to fulfill required performance of the barrier system.

The effects of fibers on the mechanical properties are considered to restrain local failure and resultantly development of failure surface by tensile forces induced in the fibers. Then, HCB is expected to keep sufficient hydraulic barrier performance when it is subjected to large deformation associated with earthquake motions and settlements of the soft foundation ground in coastal landfill sites.

In the present study, to clarify quantitatively the hydraulic barrier performance of HCB in relation to strain levels, a series of hydraulic conductivity tests were conducted on HCB specimens that had suffered from relatively large strains triaxial compression states. The same tests on CTC specimens were also conducted to compare the effects of fiber inclusion.

## 2 EXPERIMENTS

### 2.1 Material properties and mixing proportion

A standard range for mixing proportion has been obtained based on the results of laboratory mixing tests, plant mixing tests and execution works in the fields (Kotake et al. 2005). That is; a) dredged marine clay processed to slurry with water contents of 150 to 250 % that correspond to approximately 2 times as large as its liquid limit, b) hardening agent or cement of 50 to 100 kg/m<sup>3</sup> that intended to fulfill its primary function to reduce permeability of clay slurry and c) polymeric fibers of approximately 1 % in volumetric ratio to unit volume of clay slurry.

The material properties of the components and the mixing proportion adopted in the present study considering the standard range were described below:

- a) For the base geomaterial the alluvial clay dredged in Osaka Bay was used. Physical properties of the clay are as follows: fine contents 89%, density of soil particle  $\rho_s = 2.64 \text{ g/cm}^3$ , liquid limit  $w_L = 103\%$ , plastic limit  $w_p = 28\%$ . The clay was processed to slurry with water content of  $w = 206\%$ .
- b) For the hardening agent, portland blast furnace slag cement was used. The additive content employed was  $C = 90 \text{ kg/m}^3$ .

c) Polyvinyl alcohol (PVA) fibers with the additive content of  $v=1\%$  were used. The properties of PVA fiber are as follows: fineness 6.92(dtex), tensile strength at break 507 (mN), elongation at break 5.8%, apparent Young's Modulus 1,960 mN/dtex). Each fiber had length of 20mm and a nearly circular cross section with an equivalent diameter of 26  $\mu\text{m}$ .

Figure 1 shows normalized stress-strain relations of HCB ( $v=1\%$ ) and CTC ( $v=0\%$ ) obtained from triaxial compression tests. It is seen in Figure 1 that HCB produced with the proper mixing proportion exhibits sufficient toughness in the post-peak states compared to CTC. The toughness of HCB can be more clearly understood from the results of unconfined compression tests (Kotake et al. 2005).

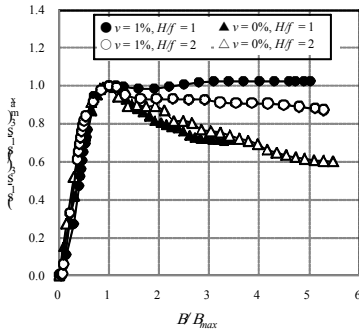


Figure 1. Normalized stress-strain relations obtained from triaxial compression tests.

## 2.2 Specimens

The cylindrical specimens of HCB and CTC were prepared according to the JGS 0821-2000 (Practice for Making and Curing Stabilized Soil Specimens without Compaction). However, the specimen size used in the present study was 50 mm in diameter and 50 mm in height. It was made shorter than an ordinary height of 100 mm so that shear bands could develop more easily to penetrate between upper and lower surfaces of the specimen.

The effects of specimen height on stress-strain relations were examined as shown in Figure 1. Comparing the case with height to diameter ratio of  $H/\phi = 1$  in the present study and the other one with  $H/\phi = 2$  in the previous work (Kotake et al. 2005), it is seen that they were very similar in the pre-peak states and that the difference in the post-peak states was relatively small.

## 2.3 Test Procedures

A triaxial compression test apparatus was used to control the mean axial strain and the confining pressures since the generation of local failure and development of shear bands in geomaterials are consi-

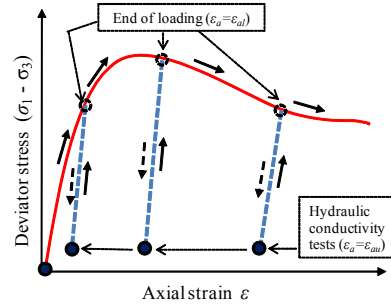


Figure 2. Controlled stress-strain relations in triaxial compression states

dered to be strongly affected by stress states. When shear bands develop to the direction where water flows in the specimen, its permeability may be increased as the water channels come to exist. However, it is difficult to control the permeability by the mean axial strain induced in the specimen due to the randomness of shear band development. Thus, the test in the present study was not considered as an element test but a kind of model test by using an ordinary triaxial compression test apparatus. The stress-strain relations of the specimens that were loaded and unloaded in triaxial compression states are schematically drawn in Figure 2.

The test procedures are described as follows:

- 1) Hydraulic conductivity test is conducted on a specimen in an initial state ( $\epsilon_a=0$ ).
- 2) The specimen is compressed vertically in undrained condition at a constant strain rate of 0.1%/min until the axial strain attains to a specific level ( $\epsilon_a=\epsilon_{al}$ ).
- 3) The specimen is unloaded at a constant strain rate of 0.1%/min to the stress state of 5-10 % of the maximum deviator stress that was applied at the end of loading ( $\epsilon_a=\epsilon_{au}$ ).
- 4) After the excess pore pressure remaining in the deformed specimen dissipates and the stress-strain reaches to a constant state ( $\epsilon_a=\epsilon_{au}$ ), hydraulic conductivity test is conducted under the confining pressure  $\sigma_c$ .
- 5) After completing the hydraulic conductivity test, the specimen is reloaded in undrained condition.
- 6) In case of hysteretic loading tests the processes from 2) to 4) are repeated.

The axial strains specified for the hydraulic conductivity tests, i.e.  $\epsilon_{al}$  were intended to correspond to those in the pre-peak state ( $\epsilon_{al}=1-3\%$ ), around the peak ( $\epsilon_{al}=3-5\%$ ) and the residual states ( $\epsilon_{al}=5-15\%$ ), respectively. The unloading process was conducted so that the specimen was able to keep in a stable state to avoid relaxation during the succeeding hydraulic conductivity test.

Figure 3 shows the schematic view of hydraulic conductivity tests using a triaxial compression test apparatus. Falling head hydraulic conductivity tests were conducted by releasing the backpressure at the bottom platen while keeping it constant at the top platen. Then, the specimen was permeated downward into an overflow tank while supplying water into the burette repeatedly as water head changed from  $h_1$  to  $h_2$ .

Test conditions for the hydraulic conductivity test are as follows: The effective confining pressure in the triaxial compression states were  $\sigma_3' = 0, 50$  and  $100 \text{ kN/m}^2$  while applying the back pressure of  $\sigma_b = 50 \text{ kN/m}^2$ . In the case of  $\sigma_3' = 0$  only membrane pressure was substantially applied to the specimen. The hydraulic conductivity tests were conducted under the confining pressure of  $\sigma_c = 50, 100$  and  $200 \text{ kN/m}^2$ . Thus, the hydraulic gradient of the 50 mm long specimens were approximately  $i = 60, 100$  and  $200$ , respectively.

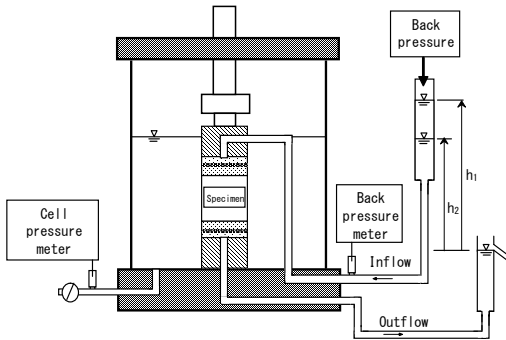


Figure 3. Outline of hydraulic conductivity test

### 3 RESULTS AND DISCUSSIONS

#### 3.1 Stress-strain relations

Figures 4 to 6 show the relationships between the deviator stress and axial strain obtained from the triaxial compression tests on HCB ( $\nu = 1\%$ ) and CTC ( $\nu = 0\%$ ) specimens that were compressed by monotonic or iterative loading under the effective confining pressures of  $50 \text{ kN/m}^2$ . It is seen that the elastic stress-strain relation during reloading is similar to the one during unloading irrespective of the strain level, and that the virgin stress-strain relation in the reloading stage is similar to the one observed in monotonically loading test.

From the test cases in that the specimens were loaded beyond the peak, it is seen that the maximum deviator stresses ( $\sigma_1 - \sigma_3$ ) of HCB were in the range from  $800$  to  $1000 \text{ kN/m}^2$  while those of CTC were from  $400$  to  $700 \text{ kN/m}^2$ . This is obviously due to the effects of fiber inclusion.

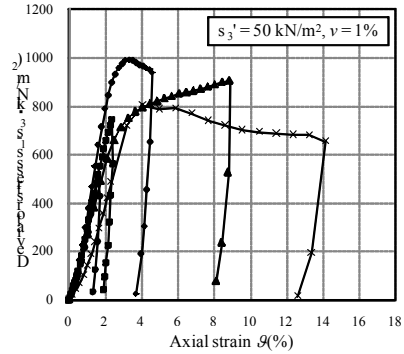


Figure 4. Stress-strain relations (HCB, monotonic)

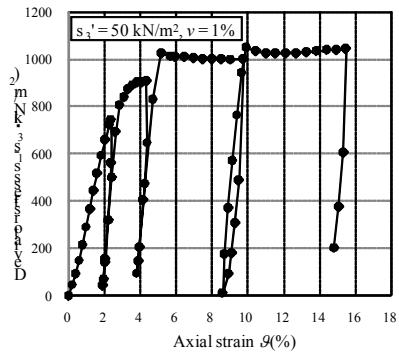


Figure 5. Stress-strain relations (HCB; iterative)

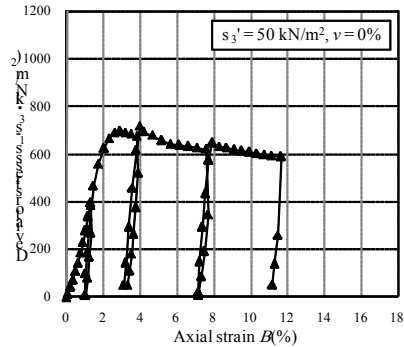


Figure 6. Stress-strain relations (CTC; iterative)

#### 3.2 Specimens after peak states

Figures 7 and 8 show the specimens of HCB and CTC respectively after hydraulic conductivity tests. The specimens were monotonically compressed to the strain levels that were around the peak state and in the post-peak state, respectively. It can be observed from the outside view that some thin failure surfaces developed diagonally and further developed as the strains increased. On the other hand, those of CTC tended to develop vertically that penetrated the

specimen and became wider as they failed under compressive stress.

It is noted that no obvious failure surfaces were observed in the specimens in that the loading processes were terminated before the peak and around the peak state (Kotake et al. 2009).

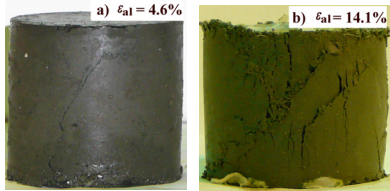


Figure 7. Specimens after tests (HCB)

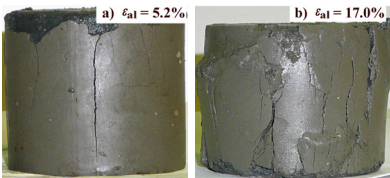


Figure 8. Specimens after tests (CTC)

### 3.3 Hydraulic conductivity

Figure 9 shows the hydraulic conductivity test results with respect to the axial strains of  $\epsilon_a = \epsilon_{al}$  in monotonic and iterative loading process under the effective confining pressure of  $\sigma_3' = 0, 50$  and  $100$  kN/m<sup>2</sup> conducted on HCB ( $\nu = 1\%$ ) and CTC ( $\nu = 0\%$ ) specimens.

- 1) The hydraulic conductivity values of HCB and CTC were approximately or less than  $k = 1.0 \times 10^{-9}$  m/s in the initial states ( $\epsilon_{al} = 0$ ). They remained almost in the initial values when the axial strains were in the range less than 4.0%.
- 2) In the test cases on HCB,  $k$  values increased by one order to  $k = 1.0 \times 10^{-8}$  m/s when the axial strains increased to 4.0-6.0% that corresponded to the peak state or slightly beyond the peak state. They afterwards remained in the similar range and kept mostly less than  $k = 1.0 \times 10^{-8}$  m/s even when the axial strains increased to the range up to  $\epsilon_{al} = 15\%$ .
- 3) In the test cases on CTC, the change of  $k$  values showed similar tendency to those of HCB when the confining pressure in loading process were  $\sigma_3' = 50$  and  $100$  kN/m<sup>2</sup>. Thus, no obvious difference due to fiber inclusion was observed here. This may attribute to the relatively low content of hardening agent that intended to prevent from appearing brittleness by expecting as low strength as possible. However, under the confining pressure of  $\sigma_3' = 0$  kN/m<sup>2</sup>, the  $k$  values increased rapidly by two order to  $k = 1.0 \times 10^{-7}$  m/s when the CTC specimen was around the peak state ( $\epsilon_{al} = 4.5\%$ ).

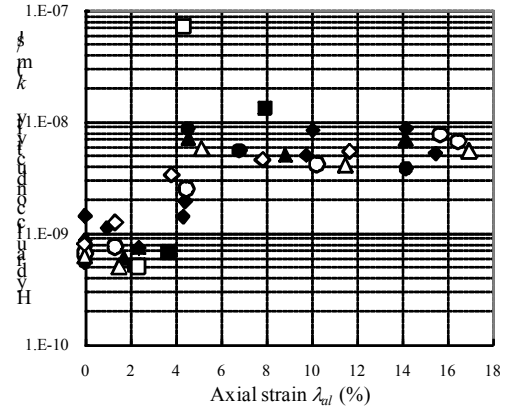
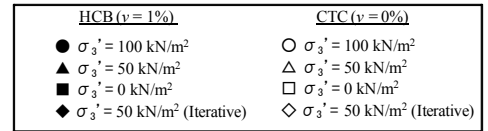


Figure 9. Hydraulic conductivity test results

## 4 CONCLUSIONS

The following conclusions were derived from the present study.

- a) The hydraulic conductivity values of HCB in the pre-peak states remained almost in the range of  $k = 1.0 \times 10^{-9}$  m/s that appeared in the initial state of zero strain, and increased by one order after the peak states, and then kept in the similar range even when the axial strains increased to the range up to  $\epsilon_{al} = 15\%$ .
- b) On the other hand, CTC showed a rapid increase in hydraulic conductivity under the low confining pressure in loading.
- c) It can be concluded that the hydraulic barrier performance of HCB are superior to CTC due to the restraining effects of local failures by fiber inclusion.

## REFERENCES

- Kotake, N., Hirata, M., Akai, T., Yamamoto, M., Ishikawa, M. and Kamon, M. 2005. Improvement of toughness of cement treated clay for barrier system by inclusion of fibrous materials. *Proc. 5th Korea-Japan Joint Seminar on Geoenvironmental Engineering*, Seoul, Korea, pp. 87-93.
- Kotake, N., Takeuchi, N., Inui, T., Katsumi, T. and Kamon, M. 2009. An Experimental Study on Hydraulic Barrier Performance of Fiber-Reinforced Cement Treated Clay in Large Strain States. *Proc. 8th Environmental Geotechnical Engineering Symposium of JGS*, pp. 129-132 (in Japanese).